

F022

3D Frequency Domain Waveform Inversion Using Time Domain Finite Difference Methods

L. Sirgue* (BP), J.T. Etgen (BP) & U. Albertin (BP)

SUMMARY

Frequency-domain waveform inversion is typically performed using frequency-domain finite-difference modelling techniques. In 3D, these methods face significant computational challenges that limit any application to full-scale seismic applications. An alternative approach is to use a 3D time-domain finite-difference method and extract the frequency-domain wavefield by computing the terms of a discrete Fourier transform at each time step. This method combines the computational efficiency of 3D time-domain modelling while permitting casting the inverse problem in the frequency domain.

Introduction

Frequency domain waveform inversion has shown great potential for the determination of high-resolution velocity model (Sirgue and Pratt, 2004; Operto et al., 2004). Because the inverse problem is cast in the frequency domain, the 2D forward problem is typically solved using an direct frequency domain modeling (Stekl and Pratt, 1998). Such approach involves the resolution of a linear system of equations (Marfurt, 1984), which leads to a predictable memory and computation complexity (George and Liu, 1981). In 2D, the frequency domain (FD) modeling is particularly efficient when many sources must be computed and in this case, turns out superior to its time domain counterpart. In its 3D formulation however, the computational burden of the FD approach becomes more dramatic (Operto et al., 2007) and make it very difficult to run on full scale problem efficiently.

In this paper, we will demonstrate how a 3D finite-difference time-domain (TD) methods may be used efficiently as an alternative modeling tool for FD waveform inversion. As proposed by Sirgue et al. (2007) and Nihei and Li (2007), we will show that a single frequency wavefield can be computed from a time marching finite difference method. We will then discuss the computational advantages of our technique over the direct 3D FD approach. We finally apply our technique to 3D waveform inversion in the SEG/EAGE overthrust model.

3D Frequency domain waveform

Waveform inversion seeks to estimate the velocity model that minimizes the data residuals waveform $\Delta\psi$ defined as the difference between the observed and the modeled data. In the frequency domain, this inversion scheme aims at minimizing the least-squares functional E and requires the computation of the 3D gradient given by:

$$\nabla E(\mathbf{x}, f) = -\text{Re} \left(\sum_s \sum_r S^* G^*(\mathbf{x}, s) G^*(\mathbf{x}, r) \Delta\psi(r, s, f) \right), \quad (1)$$

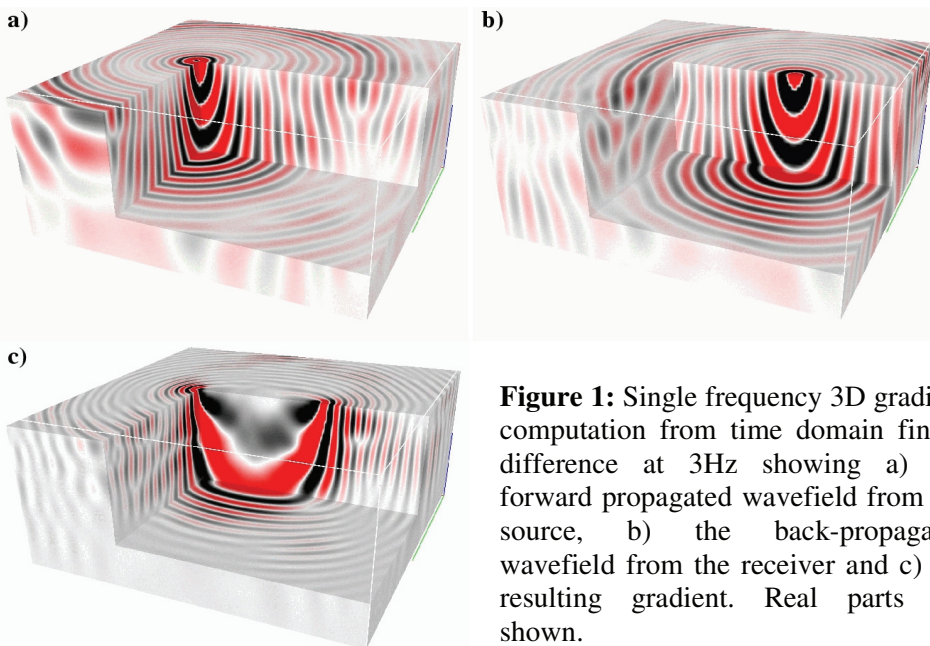


Figure 1: Single frequency 3D gradient computation from time domain finite-difference at 3Hz showing a) the forward propagated wavefield from the source, b) the back-propagated wavefield from the receiver and c) the resulting gradient. Real parts are shown.

where S is the source term, $G(\mathbf{x}, s)$ and $G(\mathbf{x}, r)$ are the single-frequency Green's functions for an excitation located at the source s and the receiver r respectively. This gradient evaluation requires the computation of two FD wavefields, a forward-propagated wavefield from the source and a backward propagated wavefield of the data residuals from the receivers. While these wavefields are typically computed using FD direct solver, we here propose their computation using a TD finite difference algorithm. The forward propagated FD wavefield is estimated by accumulating the discrete Fourier transform terms during the time marching computation of the TD wavefield such as:

$$G(f, \mathbf{x}) = \sum_{t=0}^{t_{\max}} \exp(2\pi ft) G(t, \mathbf{x}), \quad (2)$$

where $G(f, \mathbf{x})$ is the FD Green's function for a frequency f , at a position \mathbf{x} in the model and $G(t, \mathbf{x})$ is the TD Green's function at a time t . An example of computation of the forward wavefield at 3Hz is shown Figure 1a. The great advantage of this approach is that the storage of the TD wavefield is not required as the FD Green's functions are computed "on-the-fly" at each time step. This considerably simplifies the computational complexity discussed in more details in the next section.

The source term $s(t)$ at time t used at each time step is given by the inverse discrete Fourier transform of the FD source term:

$$S(t) = \exp(-2\pi ft) S(f). \quad (3)$$

The same principle is applied to the computation of the back-propagated wavefield (Figure 1b) where the FD data residuals are turned into a TD source term and the back-propagated wavefield is computed after equation (2). The resulting gradient is computed using equation 1 and is shown for a frequency of 3Hz Figure 1c.

Computational aspects

A review of the computational complexity of TD and FD methods is shown Table 1 after Nihei and Li (2007). In the 2D case, the resolution of the linear system of equations for the direct FD methods leads to a memory complexity of $O(n^2 \log_2 n)$ and a number of operations of $O(n^3)$ for a discrete model of size $n \times n$ (George and Liu, 1981). On the other hand, the TD approach corresponds to a lesser storage requirement of $O(n^2)$ but the number of operations given by $O(n^3 \cdot N_s)$ is linear with the number of sources. Since memory storage of the order of n^2 is not a problem on current architectures, the direct FD method is more advantageous than a TD method as it is very efficient for the computation of multiple sources

Finite Difference Frequency Response Modeling	Frequency Domain (single source)	Time Domain (Ns sources)
2D Storage	$O(n^2 \log_2 n)$	$O(n^2)$
2D Operations	$O(n^3)$	$O(n^2 \cdot N_t \cdot N_s) \sim O(n^3 \cdot N_s)$
3D Storage	$O(n^4)$	$O(n^3)$
3D Operations	$O(n^6)$	$O(n^3 \cdot N_t \cdot N_s) \sim O(n^4 \cdot N_s)$

Table 1: Storage and number of operation requirements for 2D ($n \times n$) and 3D ($n \times n \times n$) source finite difference frequency response modeling. After Nihei and Liu (2007).

(Marfurt, 1981).

In 3D, the computational burden of FD methods becomes more dramatic as Operto et al. (2007) showed that such problem leads to memory requirements of $O(35n^4)$ and a number of operations of $O(n^6)$ for $n \times n \times n$ model. Yet, this estimation does not account for the additional computational cost of solving for multiple sources which is, in principle, quite efficient but may turn costly when several thousands of sources must be computed.

For the 3D TD method, the memory storage is $O(n^3)$ with a number of operations of approximately $O(n^4 \cdot N_s)$. It is clear that the TD approach is more advantageous with respect to both memory storage and number of operations.

3D Waveform Inversion results

We apply our 3D FD waveform inversion to the SEG/EAGE overthrust velocity model (Figure 2a) in which 1521 sources were modeled every 500m in the inline (X) and crossline (Y) directions. Free surface multiples are present in the wavefield as well as internal multiples. A single wide-azimuth survey was generated limiting the inline and crossline offset to a maximum of 8km. The starting velocity model used for this inversion tests is a smoothed version of the true model and is shown Figure 2b. The inversions were carried out using a single frequency at a time, starting from 3 Hz and sequentially inverting for 4 then 5 Hz. For each inversion, a depth slice at $z = 2.7$ km and a cross-section at $y = 10$ km are shown. The depth slice at 2.7 km depth was chosen to display the lateral variation of the thrusted region as well as a channel complex. The channel complex in particular demonstrates the quality of the horizontal resolution and accuracy that can be recovered by 3D waveform inversion.

Figure 3 shows the results of this 3D waveform inversion and shows, as expected, an increase of resolution as higher frequency are inverted. A full comparison of different acquisition settings (Narrow versus wide azimuth) can be found in Sirgue et al. (2007).

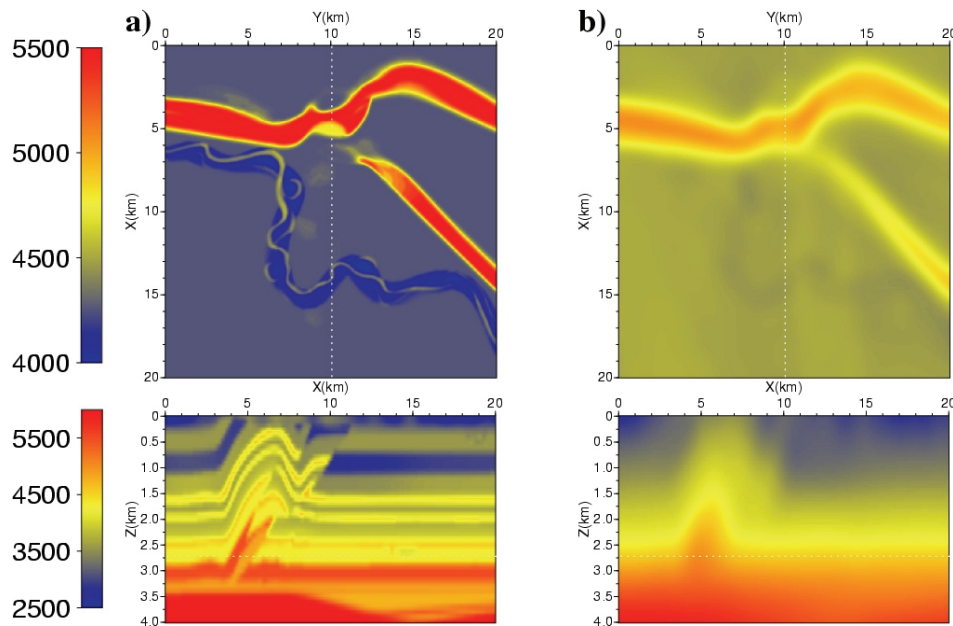


Figure 2: Depth slice at $z = 2.7$ m and cross-section at $y = 10$ km.: a) 3D True Overthrust velocity model, b) Starting velocity model used for the inversion.

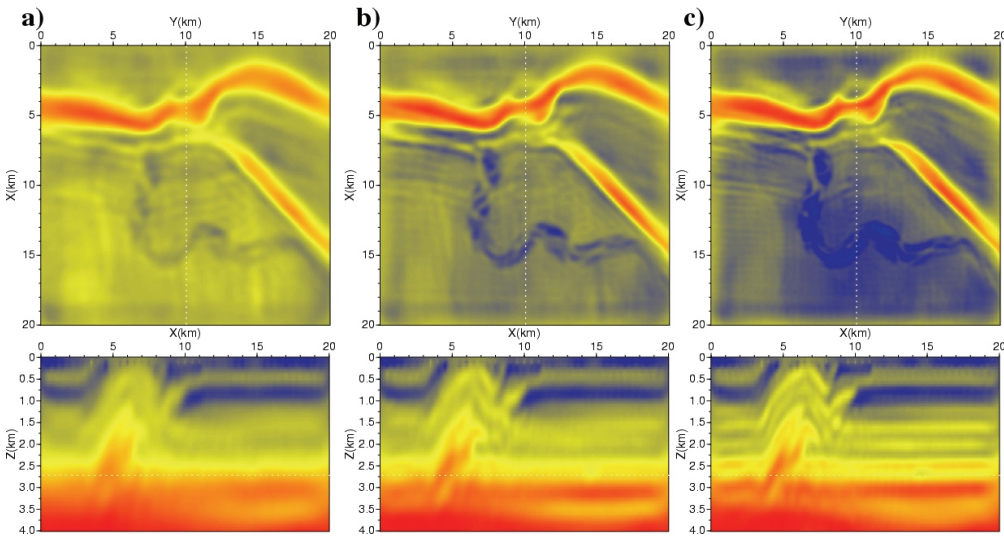


Figure 3: Wide-Azimuth acquisition. 3D waveform inversion results after a) 3Hz, b) 3 and 4 Hz and c) 3,4 and 5 Hz.

Conclusions

We have shown that time domain finite difference method can be used efficiently as a propagation engine for frequency domain waveform inversion. In 3D, the time domain modeling is more efficient than the direct frequency domain approach. This makes possible the application of 3D waveform inversion on full-scale seismic applications.

References

- George, J.A. & Liu, J.W.H. [1981] Computer Solution of Large Sparse Positive Definite Systems, Prentice-Hall, New Jersey.
- Marfurt, K.J. [1984] Accuracy of finite difference and finite element modeling of the scalar and elastic wave equations, *Geophysics*, 49, 533-549.
- Nihei, K. T., Li, X., Frequency response modelling of seismic waves using finite difference time domain with phase sensitive detection (TD-PSD), *Geophys. J. Int.*, 169, 2008.
- S. Operto, C. Ravaut, L. Imrota, J. Virieux, A. Herrero and P. Dell'Aversana [2004] Quantitative imaging of complex structures from dense wide-aperture seismic data by multiscale traveltimes and waveform inversions: a case study. *Geophysical Prospecting*, 52, 625-651.
- S. Operto, J. Virieux, P. Amestoy, J. -Y. L'Excellent, L. Giraud and H. Ben Hadj Ali [2007] 3D finite-difference frequency-domain modeling of visco-acoustic wave propagation using a massively parallel direct solver: a feasibility study, *Geophysics*, 72(5), SM195-SM211.
- Sirgue, L., and R.G. Pratt, 2004, Efficient waveform inversion and imaging: A strategy for selecting temporal frequencies: *Geophysics*, 69 , no.1, 231-248.
- Sirgue, L., Etgen, T. J., Albertin, U. and Brandsberg-Dahl, S. [2007] System and Method for 3D Frequency-Domain Waveform Inversion based on 3D Time-Domain Forward modeling, US Patent Application Publication, US2007/0282535 A1.
- Sirgue, L., Etgen, T. J., Albertin, U. [2007] 3D Full Waveform Inversion: Wide versus Narrow Azimuth Acquisitions, 77th Annual International Meeting, SEG, Expanded Abstracts.

Acknowledgments

The authors thank BP form permission to publish this work.